Remote Sensing of Environment xxx (2011) xxx–xxx

Contents lists available at SciVerse ScienceDirect

Remote Sensing of Environment

journal homepage: www.elsevier.com/locate/rse

Comparison of different vegetation indices for the remote assessment of green leaf area index of crops

Andrés Viña [a,*], Anatoly A. Gitelson [b], Anthony L. Nguy-Robertson [b], Yi Peng [b]

[a] Center for Systems Integration and Sustainability, Department of Fisheries and Wildlife, Michigan State University, East Lansing, MI, USA
[b] School of Natural Resources, University of Nebraska-Lincoln, Lincoln, NE, USA

ARTICLE INFO

Article history:
Received 20 October 2010
Received in revised form 9 August 2011
Accepted 12 August 2011
Available online xxxx

Keywords:
Chlorophyll indices
Green LAI
Maize
Soybean

ABSTRACT

Many algorithms have been developed for the remote estimation of biophysical characteristics of vegetation, in terms of combinations of spectral bands, derivatives of reflectance spectra, neural networks, inversion of radiative transfer models, and several multi-spectral statistical approaches. However, the most widespread type of algorithm used is the mathematical combination of visible and near-infrared reflectance bands, in the form of spectral vegetation indices. Applications of such vegetation indices have ranged from leaves to the entire globe, but in many instances, their applicability is specific to species, vegetation types or local conditions. The general objective of this study is to evaluate different vegetation indices for the remote estimation of the green leaf area index (Green LAI) of two crop types (maize and soybean) with contrasting canopy architectures and leaf structures. Among the indices tested, the chlorophyll Indices (the CI_{Green}, the $CI_{Red\text{-}edge}$ and the MERIS Terrestrial Chlorophyll Index, MTCI) exhibited strong and significant linear relationships with Green LAI, and thus were sensitive across the entire range of Green LAI evaluated (i.e., 0.0 to more than 6.0 m^2/m^2). However, the $CI_{Red\text{-}edge}$ was the only index insensitive to crop type and produced the most accurate estimations of Green LAI in both crops (RMSE = 0.577 m^2/m^2). These results were obtained using data acquired with close range sensors (i.e., field spectroradiometers mounted 6 m above the canopy) and an aircraft-mounted hyperspectral imaging spectroradiometer (AISA). As the $CI_{Red\text{-}edge}$ also exhibited low sensitivity to soil background effects, it constitutes a simple, yet robust tool for the remote and synoptic estimation of Green LAI. Algorithms based on this index may not require re-parameterization when applied to crops with different canopy architectures and leaf structures, but further studies are required for assessing its applicability in other vegetation types (e.g., forests, grasslands).

1. Introduction

The ratio of leaf surface area to unit ground surface area, called leaf area index (LAI) (Breda, 2003), describes the potential surface area available for leaf gas exchange between the atmosphere and the terrestrial biosphere (Cowling and Field, 2003). Therefore, it is an important parameter controlling many biological and physical processes of the vegetation, including the interception of light and water (rainfall and fog), attenuation of light through the canopy, transpiration, photosynthesis, autotrophic respiration, and carbon and nutrient (e.g. nitrogen, phosphorus, etc.) cycles. LAI obtained across a range of spatial scales, from individual plants to entire regions or continents (Bonan, 1993; Running, 1990; Running and Coughlan, 1988; Sellers et al., 1986) has been used extensively in interactive models of land surface processes (Field and Avissar, 1998; Pielke et al., 1998). As with other canopy structural properties, LAI can be separated into its photosynthetic and non-photosynthetic components. The portion of LAI composed of green leaf area (i.e., Green LAI) is the photosynthetically functional component.

Two main types of approaches have been developed to estimate Green LAI remotely: (1) inversions of canopy radiative transfer models (Fang et al., 2003; Knyazikhin et al., 1998a, 1998b; Weiss et al., 1999); and (2) empirical relationships between Green LAI and spectral vegetation indices (Chen and Cihlar, 1996; Curran, 1983a, b; Jordan, 1969; Myneni et al., 1997; Wiegand et al., 1979). While the two approaches are quite complementary (Pinty et al., 2009), it is difficult to obtain optimal parameterized solutions for radiative transfer model inversions (Fang et al., 2003). Therefore, vegetation indices have seen a more widespread use due to their ease of computation.

Spectral vegetation indices are mathematical combinations of different spectral bands mostly in the visible and near infrared regions of the electromagnetic spectrum. These numerical transformations are semi-analytical measures of vegetation activity and have been widely shown to vary not only with the seasonal variability of green foliage,

* Corresponding author at: Center for Systems Integration and Sustainability, 1405 S. Harrison Road, Suite 115 Manly Miles Bldg., Michigan State University, East Lansing, MI 48823-5243, USA. Tel.: +1 517 432 5078; fax: +1 517 432 5066.
E-mail address: vina@msu.edu (A. Viña).

0034-4257/$ – see front matter © 2011 Elsevier Inc. All rights reserved.
doi:10.1016/j.rse.2011.08.010

but also across space, thus suitable for detecting within-field spatial variability (i.e., useful in precision agriculture). The main purpose of spectral vegetation indices is to enhance the information contained in spectral reflectance data, by extracting the variability due to vegetation characteristics (e.g. LAI, vegetation cover) and to minimize soil, atmospheric, and sun-target-sensor geometry effects (Moulin and Guerif, 1999). Spectral vegetation indices constitute a simple and convenient approach to extract information from remotely sensed data, due to their ease of use, which facilitates the processing and analysis of large amounts of data acquired by satellite platforms (Govaerts et al., 1999; Myneni et al., 1995). Significant advances have been achieved in the understanding of the nature and proper interpretation of spectral vegetation indices (Myneni et al., 1995; Pinty et al., 1993) and theoretical frameworks have been proposed to support the development of indices optimized for particular applications/sensors (Gobron et al., 2000; Verstraete et al., 1996).

Applications of vegetation indices have ranged from leaf to global levels, and in the case of Green LAI, some successes have been obtained for different crops (Boegh et al., 2002; Broge and Mortensen, 2002; Clevers, 1989; Colombo et al., 2003; Curran, 1983a, b; Xiao et al., 2002). However, most vegetation indices tend to be species specific and therefore, are not robust when applied across different species, with different canopy architectures and leaf structures. The goal of this study is to evaluate the suitability of different vegetation indices for the remote estimation of multi-temporal Green LAI of crops with contrasting leaf structures and canopy architectures.

2. Methods

2.1. Study area

The study took advantage of an established research facility, which is part of the Carbon Sequestration Program at the University of Nebraska-Lincoln Agricultural Research and Development Center (UNL-ARDC). This research facility is located 58 km northeast of Lincoln, NE, U.S.A., and consists of three agricultural fields (Fig. 1). The first two (Fields 1 and 2, respectively) are 65-ha fields equipped with center pivot irrigation systems. Field 3 is of approximately the same size, but relies entirely on rainfall. All three fields were uniformly tilled prior to the initiation of the research program in 2001 and since then, Field 1 has been continuously under maize, while Fields 2 and 3 have been under a maize–soybean rotation. Prior to the initiation of the research program, there was a ten-year history of maize–soybean rotation under no till in Fields 1 and 2 (Suyker et al., 2004; Verma et al., 2005), while Field 3 had a variable cropping history of primarily wheat, soybean, oats and maize grown in 2–4 ha plots under conventional tillage (Suyker et al., 2004). The soils of the research facility are deep silty clay loam consisting of the Tomek, Yutan, Filbert, and Filmore soil series (Verma et al., 2005).

2.2. Crop cultural practices

During the growing season of 2001, the three fields were planted at the beginning of May with maize (*Zea mays* L.). A Bt corn borer resistant hybrid (Pioneer brand 33P67) was planted in Fields 1 and 2, following an east–west row direction. One day following planting, nitrogen fertilizer was applied at a rate of 128 kg N ha^{-1}. In addition to this application, 34 kg N ha^{-1} were also applied at two different occasions through the pivot. Both source and timing of N applications were chosen to minimize N_2O losses (Breitenbeck and Bremner, 1986; Eichner, 1990). Herbicide/pesticides were applied in accordance with standard practices prescribed for production scale maize ecosystems. Water application was determined based on crop water budget, by using predicted crop water use and daily monitoring of rainfall, irrigation, soil evaporation, and soil moisture, maintaining a minimum soil moisture availability of 50% within the root depth zone. For Field 3 (i.e., rainfed), a Bt hybrid (Pioneer brand 33B51) was planted in an east–west row direction. Nitrogen fertilizer was applied to Field 3 in a similar way as in Fields 1 and 2, one day following planting at a rate of 106 kg N ha^{-1}. During the 2002 growing season, only Field 1 was planted with maize (using the same hybrid and cultural practices of the 2001 growing season), while Fields 2 and 3 were planted with a soybean (*Glycene max* L.) hybrid (Asgrow 2703 Roundup Ready), also following an east–west row direction. As with maize,

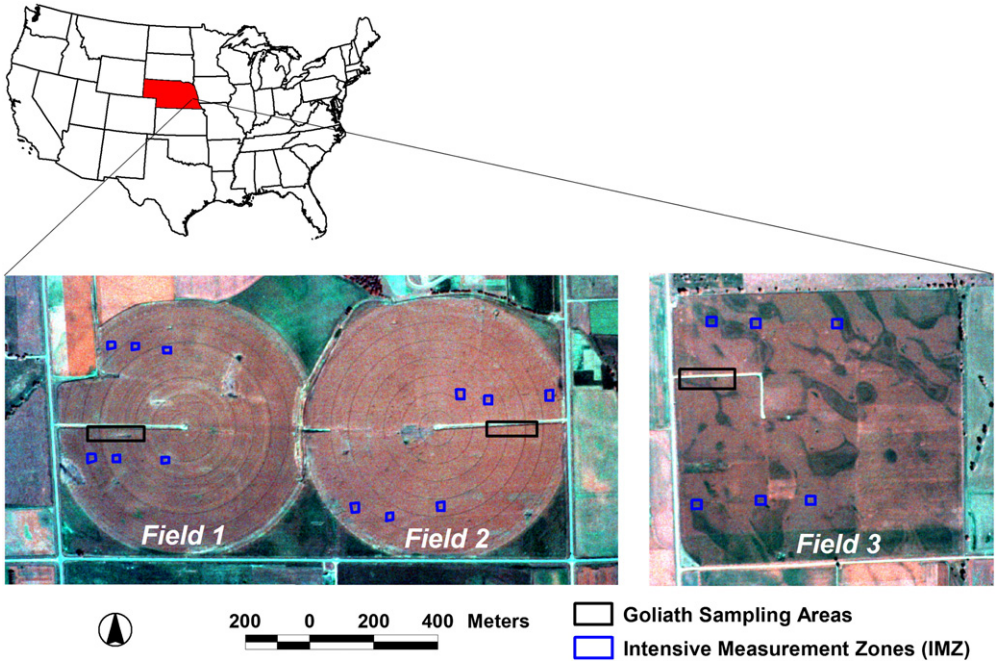

Fig. 1. Location of the field test sites at the University of Nebraska-Lincoln's Agricultural Research and Development Center (UNL-ARDC). Field 1 corresponds to irrigated continuous maize, Field 2 corresponds to irrigated maize–soybean rotation and Field 3 corresponds to rainfed maize–soybean rotation. Also shown are the locations of the Intensive Measurement Zones (IMZ) where destructive Green LAI measurements took place, and of the areas were close-range spectral measurements (i.e., with the "Goliath" all-terrain sensor platform) were acquired. Images are aerial digital multispectral images (false color composites) taken in September 10, 2001.

Please cite this article as: Viña, A., et al., Comparison of different vegetation indices for the remote assessment of green leaf area index of crops, *Remote Sensing of Environment* (2011), doi:10.1016/j.rse.2011.08.010

water application in Field 2 was determined based on crop water budget, by using predicted crop water use and daily monitoring of rainfall, irrigation, soil evaporation, and soil moisture. Herbicide/pesticides were applied in accordance with standard practices prescribed for soybean cropping systems. During the 2003 growing season, the three fields were planted with a different hybrid of maize (i.e. Pioneer 33B51BT). During the 2004 growing season, Field 1 was planted with the same maize hybrid as in 2003, while Fields 2 and 3 were planted with the same soybean hybrid as in 2002. Cultural practices for both crops remained the same for the 2003 and 2004 growing seasons.

2.3. Spectral reflectance measurements

Spectral measurements were carried out along the pivot roads of Fields 1 and 2 and along an entrance road in Field 3 (Fig. 1). Measurements were acquired during the 2001 growing season from the beginning of June until the beginning of October (18 campaigns); and in 2002, 2003 and 2004 growing seasons, from the beginning of May until the beginning of October (31, 34 and 32 campaigns in 2002, 2003, and 2004, respectively). Data in the range 400–900 nm with a sampling interval of 0.3 nm and a spectral resolution of around 1.5 nm were obtained using a dual-fiber optics system (i.e., two Ocean Optics USB2000 radiometers) mounted on "Goliath", an all-terrain sensor platform (Rundquist et al., 2004). One radiometer was equipped with a 25° field-of-view optical fiber and was placed pointed downward to measure the upwelling radiance of crops ($L_{\lambda crop}$). The height above the top of the canopy (i.e., ~5.5 m) of this radiometer was kept constant throughout the growing season, yielding a sampling area with a diameter of ~2.4 m. The second radiometer was equipped with a cosine diffuser (i.e., yielding a hemispherical field of view) and was pointed upward to simultaneously measure incident irradiance ($E_{\lambda inc}$). To match the transfer functions of these two radiometers, it was necessary to inter-calibrate them. This was accomplished by measuring the upwelling radiance ($L_{\lambda cal}$) of a white Spectralon reflectance standard (Labsphere, Inc., North Sutton, NH) simultaneously with incident irradiance ($E_{\lambda cal}$). Percent reflectance (ρ_λ) was then computed as:

$$\rho_\lambda = \left(\frac{L_{\lambda crop}}{E_{\lambda inc}}\right) \times \left(\frac{E_{\lambda cal}}{L_{\lambda cal}}\right) \times 100 \times \rho_{\lambda cal}. \quad (1)$$

Where $\rho_{\lambda cal}$ is the reflectance of the Spectralon panel linearly interpolated to match the band centers of the radiometers. A critical issue with regard to this radiometer inter-calibration is that the transfer functions (describing the transformation from radiance or irradiance collected by the sensor, to the digital counts registered) of both radiometers must be invariant through time, and minimally affected by changes in environmental conditions (e.g. temperature). The two radiometers were thus tested under field conditions (with changing illumination angles) and it was found that over a four-hour period (10:20–14:20) the coefficient of variation of the ratio of the transfer functions of the radiometers did not exceed 5% (Fig. 2).

The two radiometers were inter-calibrated immediately before and immediately after measurements in each field. To mitigate the impact of solar elevation on radiometer inter-calibration, the anisotropic reflectance from the calibration target was corrected under sunny conditions. This correction consisted in the application of general calibration equations for the directional/directional reflectance of the Spectralon reflectance standard used (Jackson et al., 1992). This correction was not performed under the diffuse light conditions characteristic of cloudy days. All data were collected with the radiometers configured to take 15 simultaneous upwelling radiance and downwelling irradiance measurements, which were internally averaged and stored as a single data file. Measurements took about 20 min per field and were collected close to solar noon (i.e., with solar angles between a minimum of 21.5° to a maximum of 54.5°).

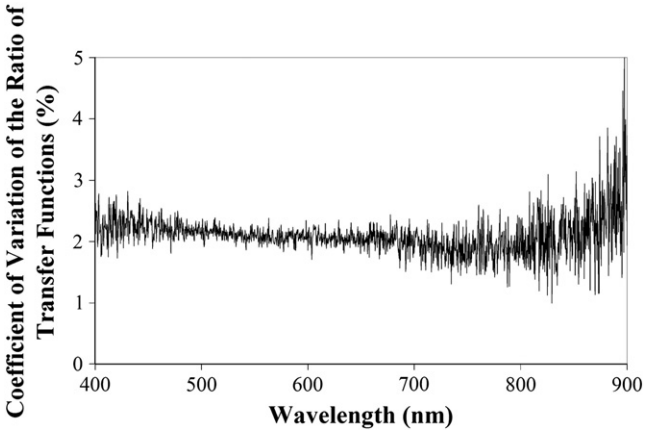

Fig. 2. Coefficient of variation (%) of the ratio of the transfer functions of the Ocean Optics USB2000 spectroradiometers in the field, over a period of 4 h (10:20–14:20).

2.4. Destructive determination of green leaf area index

Within each of the three study fields, six small (20 × 20 m) plot areas were established (Fig. 1) for performing detailed measurements. These intensive measurement zones (IMZ) represent all major occurrences of soil and crop production zones within each field (Verma et al., 2005). LAI (separated into total and green components) for each of the IMZ was obtained destructively every 2 weeks since around June 1 of every sampling year, using the following procedures: In every sampling date (i.e., nine in 2001, eight in 2002 and 2003, and nine in 2004 growing seasons) plant populations were determined (by counting plants) in each IMZ. Subsequently, six (±2) plants from a 1 m length of either of two rows within each IMZ were collected in each sampling date. Collection rows were alternated on successive dates to minimize edge effects on subsequent plant growth. Plants were transported on ice to the laboratory where they were dissected into green leaves, dead leaves, stems, and reproductive organs. Leaves were run through an area meter (Model LI-3100, Li-Cor, Inc., Lincoln NE) and the total leaf area, as well as the green leaf area per plant, was determined. For each IMZ, the total and green leaf areas per plant were multiplied by the plant population (# plants m^{-2}) to obtain a total LAI and a Green LAI. LAI values for the six IMZs were averaged to obtain a site-level value.

Table 1
Summary statistics of canopy biophysical characteristics of maize and soybean acquired in-situ during the growing seasons of 2001–2004.

		Rainfed		Irrigated	
		Maize	Soybean	Maize	Soybean
Green LAI (m^2/m^2)	Mean	2.8	2.0	4.0	2.9
	Standard Deviation	1.3	0.9	1.8	1.8
	Minimum	0.2	0.2	0.0	0.2
	Maximum	4.3	3.0	6.1	5.5
Total LAI (m^2/m^2)	Mean	3.2	2.1	4.3	3.3
	Standard Deviation	1.2	0.9	1.9	1.9
	Minimum	0.2	0.2	0.0	0.2
	Maximum	4.3	3.2	6.4	5.6
Green leaf biomass ($kg.ha^{-1}$)	Mean	1727.3	949.9	2297.1	1144.9
	Standard Deviation	849.2	476.1	1113.2	701.2
	Minimum	77.4	83.4	8.9	75.0
	Maximum	2622.2	1444.6	3636.8	2113.8
Total aboveground biomass (Dry weight; $kg.ha^{-1}$)	Mean	7465.7	3514.7	9952.4	4852.9
	Standard Deviation	4766.9	2572.6	7876.3	3927.1
	Minimum	110.1	127.0	11.4	113.9
	Maximum	14,229.7	7845.3	25,865.1	11,065.8

Table 1 shows summary statistics of the total and Green LAI measured, as well as of green leaf biomass and total above ground biomass.

As sampling dates of destructive Green LAI estimates were fewer and did not always coincide with those of canopy spectral measurements (Section 2.3 above), Green LAI values obtained destructively were interpolated to match the dates of canopy spectral measurements. For this, a weighted-linear interpolation between each pair of successive dates of Green LAI collection was defined as:

$$X_i = \frac{(t-i)\cdot X_s + (i-s)\cdot X_t}{(t-s)} \quad (2)$$

where X_s and X_t are the measured values of Green LAI on dates s and t, respectively, with $t>s$, and X_i is the interpolated Green LAI value on date i, with $s<i<t$.

2.5. Computation of spectral vegetation indices and their use for remotely estimating Green LAI

Canopy spectral reflectance data were used for calculating eight vegetation indices, many of which have been proposed as surrogates for Green LAI estimation (Broge and Leblanc, 2001; Broge and Mortensen, 2002). The vegetation indices tested include (Table 2): the Simple Ratio, SR (Jordan, 1969), the Normalized Difference Vegetation Index, NDVI (Rouse et al., 1974), the Enhanced Vegetation Index, EVI (Huete et al., 1996, 1997), the Green Atmospherically Resistant Vegetation Index, GARI (Gitelson et al., 1996), the Wide Dynamic Range Vegetation Index, WDRVI (Gitelson, 2004), the green and red-edge chlorophyll indices, CI_{Green} and $CI_{Red\text{-}edge}$, respectively (Gitelson et al., 2003a, 2003c; Gitelson et al., 2005), and the MERIS Terrestrial Chlorophyll Index, MTCI (Dash and Curran, 2004).

The NDVI, EVI, GARI, WDRVI, SR, and CI_{Green} were calculated using simulated reflectance bands of the Moderate Resolution Imaging Spectrometer, MODIS (blue: 459–479 nm, green: 545–565 nm, red: 620–670 nm, NIR: 841–876 nm) onboard NASA's Terra and Aqua satellites. The $CI_{Red\text{-}edge}$ and the MTCI were calculated using the simulated reflectance bands of the Medium Resolution Imaging Spectrometer (MERIS) onboard the European Space Agency's (ESA) Envisat satellite (i.e., red: 677.5–685 nm; red-edge: 704–714 nm; NIR: 771.25–786.25 nm and 750–757.5 nm). We chose to use these broad spectral bands because they are characteristic of two of the most currently used satellite sensor systems. In addition, Green LAI estimation using data from these systems may be more affected by mixed pixel effects (i.e., potentially including different species within a single pixel) as their spatial resolution is relatively coarse (i.e., 250–1000 m/pixel).

Best-fit linear and non-linear models between vegetation indices and Green LAI were obtained using data acquired during the 2001, 2002, 2003 and 2004 growing seasons. A factorial analysis of variance of the residuals (after checking normality and variance homogeneity) of these linear and non-linear regression models was performed in order to test if significant effects were induced by crop type (i.e., maize vs. soybean) or by field type (i.e., irrigated vs. rainfed), as well as potential interactive effects between these two factors. The linear and non-linear functions were then inverted in order to generate empirical predictive models of Green LAI, which were subsequently validated.

For model validation, we used a k-fold cross-validation procedure in which the entire data set (i.e., 261 samples) acquired between 2001 and 2004, and including both maize and soybean grown in irrigated and rainfed fields, was divided into k mutually exclusive groups following a k-fold cross-validation partitioning design (Kohavi, 1995). In our case the data were randomly split into $k=10$ sets, nine of which were used iteratively for calibration and the remaining set for validation. All eight vegetation indices tested used the same k-fold partitions. The advantages of this cross-validation method are that it reduces the dependence on a single random partition into calibration and validation data sets, and that all observations are used for both training and validation, with each observation used for validation exactly one time. Estimates (i.e., mean ± 95% confidence intervals) of model coefficients, coefficients of determination, and Root Mean Square Errors (RMSE) were obtained from this k-fold cross-validation procedure.

2.6. Field homogeneity analysis

Since the IMZ did not correspond to the close-range spectral reflectance sampling areas (Fig. 1), it was necessary to test whether these different sampling areas were comparable on a timely basis. For this, we used images acquired during the growing season of 2002 (in June 21, June 27, July 12, July 15, September 7 and September 17) by the AISA system onboard CALMIT's Piper Saratoga aircraft. The AISA is a spectrally programmable hyperspectral pushbroom imaging system, with 35 spectral bands collecting radiometric data between 480 and 860 nm. The aircraft was flown at an altitude that allowed a spatial resolution of ~3 m/pixel. All images were geometrically and radiometrically corrected. The geometric correction was obtained based on synchronizations with the navigational systems of the plane (i.e., roll, pitch, heading, and flight altitude for each data line), built-in geographic look-up tables and digital elevation models, while the radiometric correction was performed using conversions of raw digital numbers to radiance through linear response functions. Because only within field variability was assessed, no atmospheric correction was applied. Both the geometric and the radiometric corrections were performed using CaliGeo, which is an interactive program that runs as a plug-in in the ENVI digital image processing package (ITT Visual Information Solutions).

Table 2
Vegetation Indices evaluated in the study.

Index	Formulation	Reference
Simple Ratio	$SR = \frac{\rho_{NIR}}{\rho_{Red}}$	(Jordan, 1969)
Normalized Difference Vegetation Index	$NDVI = \frac{\rho_{NIR}-\rho_{Red}}{\rho_{NIR}+\rho_{Red}}$	(Rouse et al., 1974)
Enhanced Vegetation Index	$EVI = 2.5\frac{\rho_{NIR}-\rho_{Red}}{1+\rho_{NIR}+6\rho_{Red}-7.5\rho_{Blue}}$	(Huete et al., 1996; 1997)
Green Atmospherically Resistant Vegetation Index	$GARI = \frac{\rho_{NIR}-[\rho_{Green}-\gamma(\rho_{Blue}-\rho_{Red})]}{\rho_{NIR}+[\rho_{Green}-\gamma(\rho_{Blue}-\rho_{Red})]}$	(Gitelson et al., 1996)
Wide-Dynamic Range Vegetation Index	$WDRVI = \frac{\alpha\cdot\rho_{NIR}-\rho_{Red}}{\alpha\cdot\rho_{NIR}+\rho_{Red}}$	(Gitelson, 2004)
Green Chlorophyll Index	$CI_{Green} = \frac{\rho_{NIR}}{\rho_{Green}}-1$	Gitelson et al., (2003a), (2003c), (2005)
Red-edge Chlorophyll Index	$CI_{Red-edge} = \frac{\rho_{NIR}}{\rho_{Red-edge}}-1$	Gitelson et al., (2003a), (2003c), (2005)
MERIS Terrestrial Chlorophyll Index	$MTCI = \frac{\rho_{NIR}-\rho_{Red-edge}}{\rho_{Red\ edge}-\rho_{Red}}$	(Dash and Curran, 2004)

Please cite this article as: Viña, A., et al., Comparison of different vegetation indices for the remote assessment of green leaf area index of crops, *Remote Sensing of Environment* (2011), doi:10.1016/j.rse.2011.08.010

As with spectral reflectance data acquired using close-range sensors onboard "Goliath" (Rundquist et al., 2004), spectral bands of the AISA system were averaged, on a per pixel basis, to simulate bands in the visible and near-infrared regions of the MODIS and MERIS systems. The broad band pixel values were then compared between the AISA pixels located in the different IMZ and those located in the close-range spectral reflectance sampling areas (Fig. 1), using a two-sample *t*-test, after checking for variance homogeneity. Fields that showed significantly different broad band radiance values between the IMZ and the close-range spectral reflectance sampling areas are considered to be heterogeneous, and thus may constitute sources of uncertainty that could reduce the accuracy of the remote estimation of Green LAI.

2.7. Sensitivity analysis

Sensitivity of the different spectral vegetation indices to detect changes in Green LAI was tested through the use of the Noise Equivalent (NE) ΔGreen LAI:

$$NE\Delta GreenLAI = \frac{RMSE\{VI \text{ vs. } LAI\}}{d(VI)/d(LAI)} \quad (3)$$

Where d(VI)/d(LAI) is the first derivative of the best-fit function of the relationship "vegetation index (VI) vs. Green LAI" with respect to Green LAI, while RMSE is the Root Mean Square Error of the best-fit function of this relationship (Govaerts et al., 1999). The NEΔGreen LAI has the advantage of allowing the direct comparison among different spectral vegetation indices, i.e., with different scales and dynamic ranges (Viña and Gitelson, 2005).

2.8. Effects of crop type on vegetation index imagery

To assess the effects of different crop types on the eight vegetation indices calculated using the AISA imagery, we compared the histograms of the distribution of vegetation index values of the entire maize and soybean fields at a time when both exhibit similar Green LAI values. Destructive sampling showed that in September 7, 2002 the per-field average Green LAI in Field 1 (i.e., irrigated maize) and Field 2 (i.e., irrigated soybean) was ca. 3.6 m^2/m^2. Therefore, this date of image acquisition was chosen.

2.9. Evaluation of soil background effects

As shown for NDVI-like indices, the difference between NIR and red reflectance is instrumental for reducing soil background effects (Pinty et al., 2009). To evaluate the potential effects of soil background on the remote estimation of Green LAI using vegetation indices that are not based on this difference (e.g., the MTCI and the $CI_{Red-edge}$), reflectance spectra of spherical and planophile canopies with different Green LAI values ranging from 0.0 to 6.0 m^2/m^2 were simulated using reflectance spectra of two contrasting soil backgrounds (i.e., dark and bright) measured in Nebraska. The simulation was performed using a semi-discrete model for the scattering of light by vegetation, the New Advanced Discrete Model (NADIM) (Gobron et al., 1997). Using these simulated canopy reflectance spectra, we calculated the MTCI and the $CI_{Red-edge}$, tested their Green LAI predictive ability under two contrasting soil backgrounds (i.e., dark and bright), and compared them against that of a soil-resistant index, the EVI. For this, we established the relationship Green LAI vs. VI using canopy reflectance simulated with the dark soil background, and used this relationship to estimate Green LAI by the VI calculated with canopy reflectance simulated using the bright soil background. Uncertainties (i.e., Root Mean Square Error — RMSE) of these Green LAI predictions were calculated.

3. Results and discussion

3.1. Evaluation of field homogeneity

Both irrigated fields were homogeneous in all dates and spectral bands, with the exception of Field 2, in which the NIR band exhibited significant differences towards the end of the growing season (Table 3). Since irrigation tends to homogenize the productivity of crop fields, these results confirmed our expectations that no statistically significant differences should be observed between the areas where Green LAI was obtained destructively (i.e., IMZs) and the close-range sampling areas in the irrigated fields. In the case of the rainfed field, significant differences were observed in all the visible bands (including the red-edge band, but not the NIR band) only on September 7 (Table 3). The rainfed field also exhibited significant differences in the blue and green bands in July 15 and in the blue band on September 17 (Table 3). The remainder of the growing season exhibited homogeneity the rainfed field. Therefore, reflectance

Table 3
Two sample *t*-test values for the comparison of means of broad spectral bands (Blue: 475–485 nm, Green: 545–565 nm, Red: 675–685 nm, Red-edge: 705–715 nm, NIR: 750–785 nm) between Goliath sampling areas and the IMZ (see Fig. 1 for locations), calculated from reflectance data acquired by the AISA system along the growing season of 2002. AISA is a hyperspectral imaging sensor system onboard CALMIT's Piper Saratoga, with a programmable set of spectral band locations and widths. Values in bold correspond to two-sample t-tests performed for unequal variances.

Field	Field type	Crop	Date	Blue	Green	Red	Red-edge	NIR
1	Irrigated	Maize	6/21/2002	0.989	1.186	1.233	1.307	0.209
			6/27/2002	**0.192**	**0.239**	0.790	0.750	1.277
			7/12/2002	1.471	1.462	1.617	1.591	0.391
			7/15/2002	0.552	0.103	1.432	0.856	1.443
			9/7/2002	**0.135**	1.076	1.699	2.099	0.889
			9/17/2002	0.995	1.358	1.828	2.090	1.119
2	Irrigated	Soybean	6/21/2002	0.190	0.751	0.496	1.130	**2.309**
			6/27/2002	0.619	0.217	0.337	0.244	0.397
			7/12/2002	0.290	0.299	0.542	0.393	0.539
			7/15/2002	0.590	0.403	0.555	0.518	0.966
			9/7/2002	0.730	1.219	1.995	1.140	4.339[§]
			9/17/2002	1.499	0.708	0.008	0.613	0.339
3	Rainfed	Soybean	6/21/2002	**1.556**	**1.285**	**0.689**	**0.910**	2.098
			6/27/2002	1.014	**0.690**	**0.043**	**0.170**	1.831
			7/12/2002	0.623	**0.716**	**0.133**	**0.067**	1.070
			7/15/2002	2.906[*]	2.553[*]	1.562	1.772	0.735
			9/7/2002	3.613[#]	3.692[#]	2.495[*]	2.367[*]	1.021
			9/17/2002	2.284[*]	0.060	2.087	0.207	2.057

[*]$p<0.05$; [#]$p<0.01$; and [§]$p<0.001$.

Please cite this article as: Viña, A., et al., Comparison of different vegetation indices for the remote assessment of green leaf area index of crops, *Remote Sensing of Environment* (2011), doi:10.1016/j.rse.2011.08.010

sampling areas were, for the most part, representative of those where destructive Green LAI data were acquired. However, data acquired during dates of significant field heterogeneity may constitute a source of uncertainty that may reduce the accuracy of the remote estimation of Green LAI.

3.2. Evaluation of vegetation indices for the estimation of Green LAI at close range

The NDVI, the EVI, the GARI, and the WDRVI exhibited asymptotic relationships with Green LAI, showing high sensitivity at low-to-

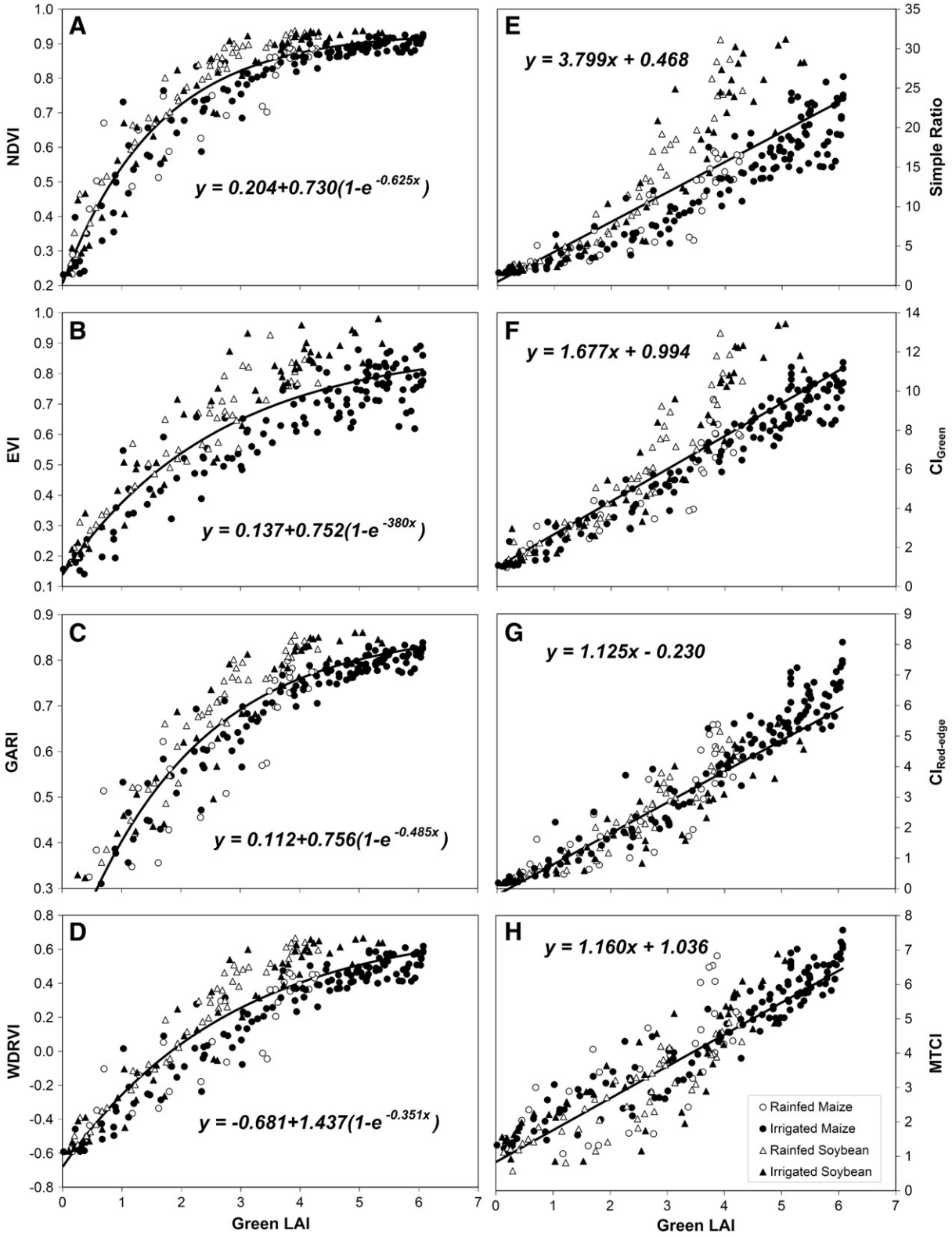

Fig. 3. Relationships between (A) NDVI, (B) EVI, (C) GARI, (D) WDRVI (E) Simple Ratio, (F) CI_{Green}, (G) $CI_{Red\text{-}edge}$, and (H) MTCI vs. Green LAI, for maize and soybean in irrigated and rainfed fields during the growing seasons of 2001–2004. Lines correspond to best fit functions.

Please cite this article as: Viña, A., et al., Comparison of different vegetation indices for the remote assessment of green leaf area index of crops, *Remote Sensing of Environment* (2011), doi:10.1016/j.rse.2011.08.010

intermediate Green LAI values that decreased considerably when Green LAI exceeded 3.0 m^2/m^2 (Fig. 3A–D). The relationship between the EVI and Green LAI exhibited a high scattering of the points from the non-linear fit (Fig. 3B). In contrast, the relationships between Green LAI vs. the Simple Ratio, the CI_{Green}, the $CI_{Red\text{-}edge}$ and the MTCI, were linear for both crops (i.e., maize and soybean) and in both irrigated and rainfed fields during the growing seasons of 2001 through 2004 (Fig. 3E–F). The relationship between the Simple Ratio and Green LAI, although linear, showed higher scattering of the sampling points from the linear fit (Fig. 3E).

A factorial analysis of variance of the residuals of the linear and non-linear models depicted in Fig. 3 showed that no significant ($p<0.05$) interaction effect was observed between field (i.e., irrigated vs. rainfed) and crop type (i.e., maize vs. soybean) for all indices evaluated (Table 4). However, all indices exhibited significantly ($p<0.05$) different residuals for maize and soybean, with the exception of the

Table 4
Factorial analyses of variance of the residuals from the best-fit functions (Fig. 3) between the vegetation indices evaluated vs. Green LAI.

Vegetation index	Factor	Factor name	Mean	Standard error	F-value	p-value
Simple Ratio	Field	Rainfed	0.711	0.404	0.02	0.879
		Irrigated	0.635	0.294		
	Crop type	Maize	−1.744	0.347	93.48	<0.0001
		Soybean	3.091	0.360		
	Crop × field	Rainfed maize	−1.527	0.619	0.51	0.475
		Rainfed soybean	2.950	0.519		
		Irrigated maize	−1.961	0.313		
		Irrigated soybean	3.231	0.498		
NDVI	Field	Rainfed	0.015	0.006	5.26	0.023
		Irrigated	−0.001	0.004		
	Crop type	Maize	−0.018	0.005	53.81	<0.0001
		Soybean	0.033	0.005		
	Crop × field	Rainfed maize	−0.015	0.009	2.37	0.125
		Rainfed soybean	0.046	0.007		
		Irrigated maize	−0.020	0.004		
		Irrigated soybean	0.019	0.006		
EVI	Field	Rainfed	−0.001	0.008	4.80	0.029
		Irrigated	0.021	0.006		
	Crop type	Maize	−0.045	0.008	107.45	<0.0001
		Soybean	0.064	0.007		
	Crop × field	Rainfed maize	−0.053	0.013	0.34	0.562
		Rainfed soybean	0.050	0.011		
		Irrigated maize	−0.036	0.006		
		Irrigated soybean	0.079	0.010		
GARI	Field	Rainfed	0.014	0.005	3.75	0.054
		Irrigated	0.001	0.004		
	Crop type	Maize	−0.017	0.005	47.55	<0.0001
		Soybean	0.031	0.005		
	Crop × field	Rainfed maize	−0.016	0.008	1.95	0.1638
		Rainfed soybean	0.043	0.007		
		Irrigated maize	−0.019	0.004		
		Irrigated soybean	0.019	0.007		
WDRVI	Field	Rainfed	0.032	0.012	2.84	0.093
		Irrigated	0.006	0.009		
	Crop type	Maize	−0.056	0.009	88.34	<0.0001
		Soybean	0.090	0.011		
	Crop × field	Rainfed maize	−0.046	0.018	1.14	0.286
		Rainfed soybean	0.111	0.016		
		Irrigated maize	−0.056	0.009		
		Irrigated soybean	0.069	0.015		
CI_{Green}	Field	Rainfed	0.243	0.135	0.29	0.593
		Irrigated	0.154	0.098		
	Crop type	Maize	−0.484	0.116	66.60	<0.0001
		Soybean	0.881	0.120		
	Crop × field	Rainfed maize	−0.401	0.207	0.21	0.648
		Rainfed soybean	0.887	0.173		
		Irrigated maize	−0.567	0.105		
		Irrigated soybean	0.875	0.167		
$CI_{Red\text{-}edge}$	Field	Rainfed	0.159	0.098	3.70	0.055
		Irrigated	−0.069	0.066		
	Crop type	Maize	0.054	0.063	0.20	0.656
		Soybean	0.013	0.066		
	Crop × field	Rainfed maize	0.151	0.114	0.56	0.453
		Rainfed soybean	0.179	0.095		
		Irrigated maize	−0.043	0.057		
		Irrigated soybean	−0.153	0.091		
MTCI	Field	Rainfed	0.097	0.096	6.37	0.012
		Irrigated	−0.202	0.070		
	Crop type	Maize	0.348	0.082	45.37	<0.0001
		Soybean	−0.453	0.085		
	Crop × field	Rainfed maize	0.465	0.147	0.30	0.582
		Rainfed soybean	−0.270	0.123		
		Irrigated maize	0.231	0.074		
		Irrigated soybean	−0.636	0.118		

Please cite this article as: Viña, A., et al., Comparison of different vegetation indices for the remote assessment of green leaf area index of crops, *Remote Sensing of Environment* (2011), doi:10.1016/j.rse.2011.08.010

$CI_{Red\text{-}edge}$ (Table 4). Therefore, with the exception of the $CI_{Red\text{-}edge}$, all vegetation indices tested may require different model coefficients for the remote estimation of Green LAI in different crop types. This means that even in such contrasting crop types with respect to leaf structure (i.e., monocotyledon vs. dicotyledon) and canopy architecture (i.e., planophile vs. spherical leaf angle distribution) as maize and soybean, the algorithm for estimating Green LAI using the $CI_{Red\text{-}edge}$ does not require re-parameterization of model coefficients. In addition, the residuals of NDVI, EVI and MTCI vs. Green LAI were significantly different between irrigated and rainfed fields (Table 4), suggesting that in order to improve the accuracy of the estimation of Green LAI obtained from these indices, different parameterizations for irrigated and rainfed conditions may also be required.

3.3. Sensitivity analysis

The sensitivity analysis was performed by estimating the Noise Equivalent ΔGreen LAI using a single parameterization (i.e., a single model for maize and soybean in irrigated and rainfed fields) of the linear and non-linear models between each vegetation index and Green LAI (Fig. 3). We used a single parameterization, in order to compare the performance of the eight indices under a mixed pixel scenario. Results of this analysis show that the NDVI and the GARI exhibited the lowest NE ΔGreen LAI values (thus the highest sensitivities to Green LAI) for Green LAI below 2.0 m^2/m^2. In contrast, the MTCI, the CI_{Green} and the $CI_{Red\text{-}edge}$ exhibited the lowest NE ΔGreen LAI values for Green LAI exceeding 3.0 m^2/m^2 (Fig. 4). The EVI and the WDRVI had higher sensitivities than the CI_{Green} and $CI_{Red\text{-}edge}$ at Green LAI<2 m^2/m^2, and higher sensitivities than the NDVI at Green LAI>2 m^2/m^2. Both of these indices exhibited almost the same NE ΔGreen LAI but the WDRVI showed slightly higher sensitivity than EVI across the entire range of Green LAI studied (Fig. 4). Therefore, NDVI and GARI are the best indices for quantitatively detecting changes in Green LAI values <2 m^2/m^2, while the MTCI, the CI_{Green} and the $CI_{Red\text{-}edge}$ are the best for detecting changes in Green LAI values >3 m^2/m^2.

3.4. Model validation

Coefficients of model inversions between Green LAI and vegetation indices are presented in Table 5. In this table, the accuracy of the remote Green LAI estimation is represented by the Root Mean Square Error, RMSE. Among the eight vegetation indices tested, the $CI_{Red\text{-}edge}$ and the MTCI exhibited the lowest RMSE, with the $CI_{Red\text{-}edge}$, exhibiting the lowest of all (RMSE = 0.577 m^2/m^2). Therefore, remote sensing metrics developed originally to estimate chlorophyll content (i.e., the $CI_{Red\text{-}edge}$ and the MTCI) can also be used for an accurate remote estimation of Green LAI of crop canopies ranging from 0.0 to more than 6.0 m^2/m^2.

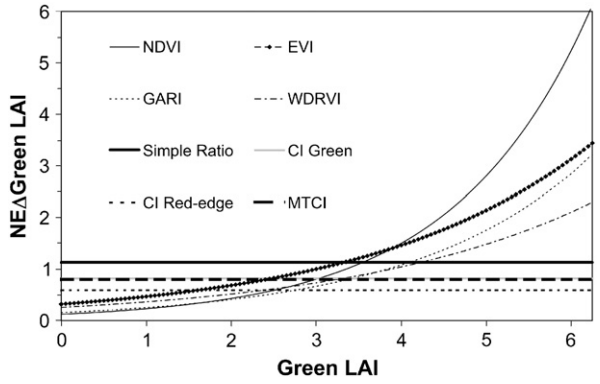

Fig. 4. Sensitivity of the different spectral vegetation indices tested to Green LAI of maize and soybean in irrigated and rainfed fields during the growing seasons of 2001 to 2004. Sensitivity was evaluated using the NE ΔLAI (Eq. 3).

Table 5
Algorithms for remotely estimating Green LAI using the eight vegetation indices evaluated. Values of the Root Mean Square Error (RMSE, m^2/m^2) represent the accuracies of the different algorithms in estimating Green LAI. All model coefficients, RMSE and their ±95% confidence intervals (in parentheses) were obtained using a *k*-fold cross validation procedure, with $k = 10$.

Model (inverted)	Y_0	a	b	RMSE
$Green\,LAI = \frac{\ln\left(\frac{1}{1-\frac{NDVI-Y_0}{a}}\right)}{b}$	0.2064	0.7298	0.6159	1.176 (0.014)
$Green\,LAI = \frac{\ln\left(\frac{1}{1-\frac{EVI-Y_0}{a}}\right)}{b}$	0.1408	0.7512	0.3789	2.533 (0.040)
$Green\,LAI = \frac{\ln\left(\frac{1}{1-\frac{GARI-Y_0}{a}}\right)}{b}$	0.3417	0.5322	0.4727	0.985 (0.013)
$Green\,LAI = \frac{\ln\left(\frac{1}{1-\frac{WDRVI-Y_0}{a}}\right)}{b}$	−0.6684	1.4392	0.3418	0.982 (0.008)
$Green\,LAI = \left(\frac{Simple\,Ratio-Y_0}{a}\right)$	0.5761	3.7880	N/A	1.095 (0.008)
$Green\,LAI = \left(\frac{CI_{Green}-Y_0}{a}\right)$	0.9910	1.6769	N/A	0.781 (0.006)
$Green\,LAI = \left(\frac{CI_{Red-edge}-Y_0}{a}\right)$	−0.1179	1.4065	N/A	0.577 (0.003)
$Green\,LAI = \left(\frac{MTCI-Y_0}{a}\right)$	1.3375	2.1366	N/A	0.682 (0.003)

3.5. Effects of crop type on vegetation index imagery

With the exception of the $CI_{Red\text{-}edge}$ image, the irrigated maize and soybean fields were discernible from each other in all the vegetation index images, and exhibited a clear separation in their histogram values (Fig. 5). These results correspond with those obtained using close-range remote sensing techniques (Table 4), in which the only index that showed no significant differences among crop types was the $CI_{Red\text{-}edge}$. In addition, for the same Green LAI all indices (excluding the $CI_{Red\text{-}edge}$) showed lower values for maize than for soybean, with the exception of the MTCI in which the soybean field exhibited lower values than those of maize (Fig. 5). The difference between MTCI in maize and in soybean may be explained by the different leaf structures and canopy architectures of these crops. On the one hand, chlorophyll content in the adaxial and abaxial sides of maize leaves are virtually the same, while in soybean leaves chlorophyll content in the adaxial side is considerably higher than in the abaxial one. On the other hand, while soybean exhibits a characteristic planophile canopy (i.e., predominantly horizontal leaves), the canopy of maize tends to exhibit a more spherical (i.e., uniform) leaf angle distribution. These main differences in foliar chlorophyll distribution and leaf angle distribution induce complex effects on the reflectance of maize and soybean canopies that directly affect the sensitivity of different vegetation indices to Green LAI. One of such complex effects is that under the same Green LAI, due to higher chlorophyll content in the adaxial surface of soybean leaves, reflectance of the soybean canopy in the red region is lower than that in the maize canopy (i.e., higher absorption by chlorophyll in soybean; Fig. 6). However, due to a higher scattering by the soybean canopy, soybean reflectance

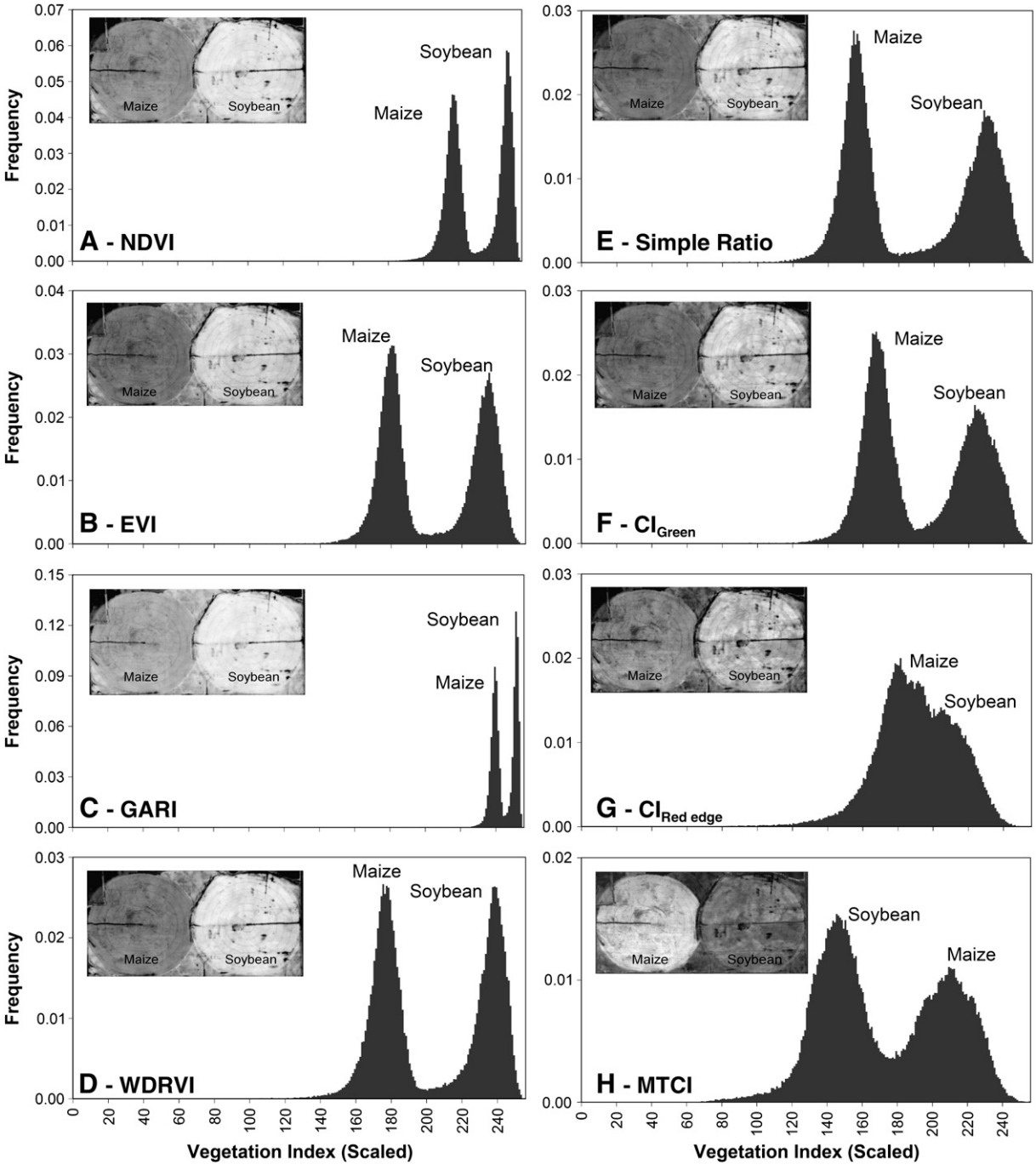

Fig. 5. Histograms showing the distribution of pixel values within the images of (A) NDVI, (B) EVI, (C) GARI, (D) WDRVI, (E) Simple Ratio, (F) CI_{Green}, (G) $CI_{Red\text{-}edge}$, and (H) MTCI. These images were calculated from an imaging overpass of the aircraft-mounted AISA sensor in September 7, 2002 over irrigated maize and soybean fields (Green LAI of around 3.6 m^2/m^2 in both fields). Insets show the respective images. Changes in image intensity depict the differential sensitivities of the indices to the two crop types evaluated. Maize and soybean fields are discernible from each other in all these images, with the exception of the $CI_{Red\text{-}edge}$ image. This demonstrates the robustness of this index for Green LAI estimation in canopies with different leaf structures and canopy architectures.

increases sharply toward longer wavelengths, reaching up to 60% at around 800 nm (Fig. 6), while maize NIR reflectance is considerably lower (up to 40%; Fig. 6). In addition, with an increase in wavelength, the depth of light penetration into the leaf increases. In the soybean leaf, it reaches the spongy layer, which has lower chlorophyll content than the palisade layer. In contrast, in the maize leaf, chlorophyll content remains the same along the leaf depth and deeper light penetration brings an increase in absorption. As a result, in the red-edge region, soybean reflectance is higher than that in maize. Thus, the difference between reflectance in the red-edge and in the red spectral regions (i.e., numerator of the MTCI) is lower in maize canopies than in soybean canopies with the same Green LAI. Contrary to the MTCI, the $CI_{Red\text{-}edge}$ values are almost the same for both maize and soybean with the same Green LAI, since although soybean shows higher values of red-edge and NIR reflectance than maize, the ratio $\rho_{NIR}/\rho_{Red\text{-}edge}$ remains almost the same (Fig. 6).

3.6. Evaluation of soil background effects

The effects of contrasting dark and bright soil backgrounds on the remote estimation of Green LAI are shown in Fig. 7. This figure shows RMSE of the remote estimation of Green LAI over a bright soil using

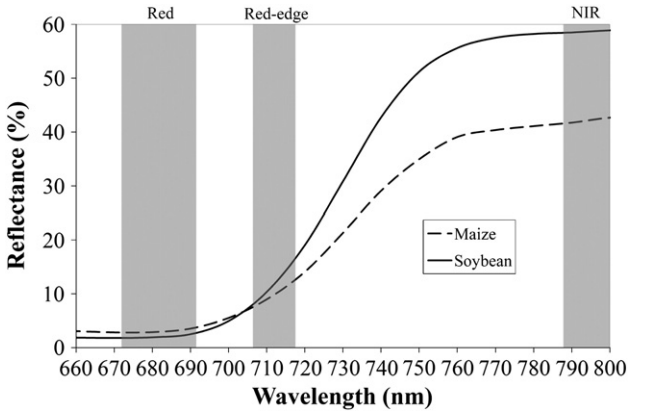

Fig. 6. Reflectance spectra of maize and soybean canopies with similar Green LAI (ca. 4.0 m^2/m^2).

the established relationship over a dark soil for the two best indices found in the study for remotely assessing Green LAI, the MTCI and the $CI_{Red\text{-}edge}$. As the EVI has been suggested to be resistant to changes in background reflectance (Huete et al., 1997), this index was also included for comparison purposes. It can be seen that while both the MTCI and the $CI_{Red\text{-}edge}$ were affected by different soil background reflectances, these indices still exhibited lower uncertainties than the soil-resistant EVI. However, the $CI_{Red\text{-}edge}$ exhibited higher uncertainty in the simulated spherical canopy while the MTCI exhibited higher uncertainty in the simulated planophile canopy. As the soil background may be more visible even under higher Green LAI values in spherical canopies than in planophile canopies, this suggests that the $CI_{Red\text{-}edge}$ may be more affected by soil background effects than the MTCI.

4. Concluding remarks

The photosynthetic component of LAI (i.e., Green LAI) has been traditionally determined using visual (i.e., subjective) attributions of the "greenness" of leaves (Boegh et al., 2002; Ciganda et al., 2008; Curran, 1983a; Gitelson et al., 2003c). Therefore, the Green LAI represents a subjective metric, as it depends on a visual inspection of the color of leaves. While a strong linear relationship exists between canopy chlorophyll content and Green LAI obtained using this subjective greenness attribution, such relationship exhibits hysteresis, particularly during the senescence period (see Fig. 1 in Peng et al., 2011). Therefore, metrics for the estimation of canopy chlorophyll content such as the MTCI (Dash and Curran, 2004), the CI_{Green} and the $CI_{Red\text{-}edge}$ (Gitelson et al., 2005), which have also been successfully related with the gross primary productivity (GPP) of vegetation canopies (Gitelson et al., 2003b; Gitelson et al., 2006; Gitelson et al., 2008; Harris and Dash, 2010; Hilker et al., 2011), may actually provide a more accurate representation of the photosynthetically active component of the LAI than destructive sampling. In this study we evaluated the sensitivity of these chlorophyll indices, together with other spectral vegetation indices, for the remote estimation of Green LAI in two crop types (i.e., maize and soybean) exhibiting contrasting leaf structures and canopy architectures.

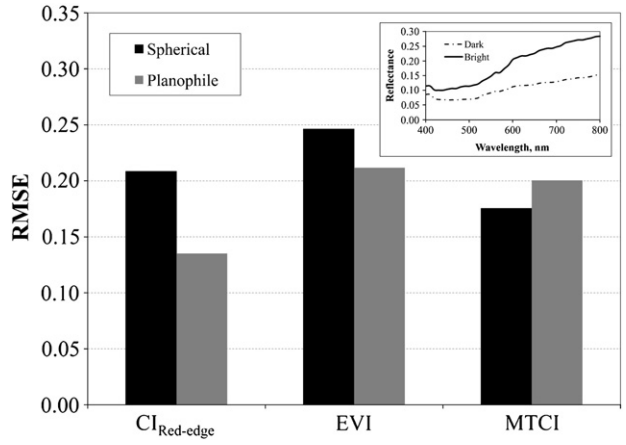

Fig. 7. Root Mean Square Error (RMSE, m^2/m^2) of Green LAI estimation (in a range of 0 to 6 m^2/m^2) in simulated spherical (i.e., uniform leaf angle distribution) and planophile (i.e., predominantly horizontal leaf angle distribution) canopies. The estimation was obtained over a bright soil background using the coefficients of the relationship between Green LAI vs. Vegetation Index established over a dark soil background. The vegetation indices shown correspond to the MTCI and the $CI_{Red\text{-}edge}$, together with a background resistant index, the EVI, for comparison purposes. The inset shows the reflectance spectra of the dark and bright soil backgrounds used in the simulations.

Among the eight indices tested, the chlorophyll indices (i.e., the CI_{Green}, the $CI_{Red\text{-}edge}$ and the MTCI) were found to be linearly related with Green LAI and thus exhibited more sensitivity to moderate-to-high Green LAI than widely used NDVI-like indices. This was expected by the linear relationship between canopy chlorophyll content and Green LAI. Through model simulations, we evaluated the sensitivity to soil background effects of the MTCI and the $CI_{Red\text{-}edge}$. The simulations showed that these two indices performed better than an established and amply used soil-background insensitive index, the EVI, suggesting that the accuracy of the MTCI and the $CI_{Red\text{-}edge}$ at predicting Green LAI was not drastically affected by soil background effects. Other sources of uncertainty, such as the spatial and temporal mismatch between the destructive sampling of Green LAI and close-range canopy spectral measurements, were also present in the study. However, these were not systematic and did not appreciably reduce the accuracy of the remote estimations of Green LAI, thus were treated as random errors.

The main conclusion of this study is that chlorophyll indices such as the MTCI and the $CI_{Red\text{-}edge}$ constitute suitable surrogates of Green LAI. These indices may even constitute better metrics than the subjectively determined Green LAI, as they objectively respond to changes in both leaf area and foliar chlorophyll content. However, it was found that the MTCI was sensitive to crop type, thus requiring re-parameterization of the algorithms for estimating Green LAI of vegetation with different canopy architectures and leaf structures. Therefore, a priori knowledge of crop type would be required for a successful application of the MTCI for Green LAI estimation in different crops types. In contrast, the $CI_{Red\text{-}edge}$ was crop type insensitive, thus may not require re-parameterization under different crop types. The $CI_{Red\text{-}edge}$ is therefore a suitable, accurate and yet inexpensive tool for the remote estimation of Green LAI at multiple scales, from close-range to entire regions and continents, using currently operational satellite sensor systems such as Hyperion and MERIS. However, further studies are required to test the suitability of the $CI_{Red\text{-}edge}$ for the remote estimation of Green LAI not only in different crop types but also in other vegetation types (e.g., forests, grasslands).

Acknowledgments

This research was partially supported by the U.S. Department of Energy: (a) EPSCoR program, Grant No. DE-FG-02-00ER45827 and (b) Office of Science (BER) Grant No. DE-FG03-00ER62996, as well as the NASA EPSCoR "Aerial" grant and the Nebraska Space Grant programs. We acknowledge the support and the use of facilities and equipment provided by the Center for Advanced Land Management Information Technologies (CALMIT), and the Carbon Sequestration Program, University of Nebraska-Lincoln. We are very grateful to Nadine Gobron for providing the simulated reflectances of spherical and planophile crop canopies, as well as to Timothy Arkebauer,

Donald C. Rundquist and Shashi B. Verma for their help and support with data collection. Finally, we also acknowledge three anonymous reviewers who provided useful comments to the manuscript.

References

Boegh, E., Soegaard, H., Broge, N., Hasager, C. B., Jensen, N. O., Schelde, K., et al. (2002). Airborne multispectral data for quantifying leaf area index, nitrogen concentration, and photosynthetic efficiency in agriculture. *Remote Sensing of Environment*, *81*, 179–193.

Bonan, G. B. (1993). Importance of leaf-area index and forest type when estimating photosynthesis in boreal forests. *Remote Sensing of Environment*, *43*, 303–314.

Breda, N. J. J. (2003). Ground-based measurements of leaf area index: A review of methods, instruments and current controversies. *Journal of Experimental Botany*, *54*, 2403–2417.

Breitenbeck, G. A., & Bremner, J. M. (1986). Effects of various nitrogen fertilizers on emission of nitrous-oxide from soils. *Biology and Fertility of Soils*, *2*, 195–199.

Broge, N. H., & Leblanc, E. (2001). Comparing prediction power and stability of broadband and hyperspectral vegetation indices for estimation of green leaf area index and canopy chlorophyll density. *Remote Sensing of Environment*, *76*, 156–172.

Broge, N. H., & Mortensen, J. V. (2002). Deriving green crop area index and canopy chlorophyll density of winter wheat from spectral reflectance data. *Remote Sensing of Environment*, *81*, 45–57.

Chen, J. M., & Cihlar, J. (1996). Retrieving leaf area index of boreal conifer forests using Landsat TM images. *Remote Sensing of Environment*, *55*, 153–162.

Ciganda, V., Gitelson, A., & Schepers, J. (2008). Vertical profile and temporal variation of chlorophyll in maize canopy: Quantitative "crop vigor" indicator by means of reflectance-based techniques. *Agronomy Journal*, *100*, 1409–1417.

Clevers, J. G. P. W. (1989). The application of a weighted infrared-red vegetation index for estimating leaf-area index by correcting for soil-moisture. *Remote Sensing of Environment*, *29*, 25–37.

Colombo, R., Bellingeri, D., Fasolini, D., & Marino, C. M. (2003). Retrieval of leaf area index in different vegetation types using high resolution satellite data. *Remote Sensing of Environment*, *86*, 120–131.

Cowling, S. A., & Field, C. B. (2003). Environmental control of leaf area production: Implications for vegetation and land-surface modeling. *Global Biogeochemical Cycles*, *17*, 1007, doi:10.1029/2002GB001915.

Curran, P. J. (1983). Estimating green LAI from multispectral aerial-photography. *Photogrammetric Engineering and Remote Sensing*, *49*, 1709–1720.

Curran, P. J. (1983). Multispectral remote-sensing for the estimation of green leaf-area index. *Philosophical Transactions of the Royal Society of London Series a—Mathematical Physical and Engineering Sciences*, *309*, 257–270.

Dash, J., & Curran, P. J. (2004). The MERIS terrestrial chlorophyll index. *International Journal of Remote Sensing*, *25*, 5403–5413.

Eichner, M. J. (1990). Nitrous-oxide emissions from fertilized soils — Summary of available data. *Journal of Environmental Quality*, *19*, 272–280.

Fang, H. L., Liang, S. L., & Kuusk, A. (2003). Retrieving leaf area index using a genetic algorithm with a canopy radiative transfer model. *Remote Sensing of Environment*, *85*, 257–270.

Field, C. B., & Avissar, R. (1998). Bidirectional interactions between the biosphere and the atmosphere — Introduction. *Global Change Biology*, *4*, 459–460.

Gitelson, A. A. (2004). Wide dynamic range vegetation index for remote quantification of biophysical characteristics of vegetation. *Journal of Plant Physiology*, *161*, 165–173.

Gitelson, A. A., Gritz, Y., & Merzlyak, M. N. (2003). Relationships between leaf chlorophyll content and spectral reflectance and algorithms for non-destructive chlorophyll assessment in higher plant leaves. *Journal of Plant Physiology*, *160*, 271–282.

Gitelson, A. A., Kaufman, Y. J., & Merzlyak, M. N. (1996). Use of a green channel in remote sensing of global vegetation from EOS-MODIS. *Remote Sensing of Environment*, *58*, 289–298.

Gitelson, A. A., Verma, S. B., Viña, A., Rundquist, D. C., Keydan, G., Leavitt, B., et al. (2003). Novel technique for remote estimation of CO_2 flux in maize. *Geophysical Research Letters*, *30*, 486, doi:10.1029/2002GL016543.

Gitelson, A. A., Viña, A., Arkebauer, T. J., Rundquist, D. C., Keydan, G., & Leavitt, B. (2003). Remote estimation of leaf area index and green leaf biomass in maize canopies. *Geophysical Research Letters*, *30*, 1248, doi:10.1029/2002GL016450.

Gitelson, A. A., Viña, A., Ciganda, V., Rundquist, D. C., & Arkebauer, T. J. (2005). Remote estimation of canopy chlorophyll content in crops. *Geophysical Research Letters*, *32*, L08403, doi:10.1029/2005GL022688.

Gitelson, A. A., Viña, A., Masek, J. G., Verma, S. B., & Suyker, A. E. (2008). Synoptic monitoring of gross primary productivity of maize using landsat data. *IEEE Geoscience and Remote Sensing Letters*, *5*, 133–137.

Gitelson, A. A., Viña, A., Verma, S. B., Rundquist, D. C., Arkebauer, T. J., Keydan, G., et al. (2006). Relationship between gross primary production and chlorophyll content in crops: Implications for the synoptic monitoring of vegetation productivity. *Journal of Geophysical Research—Atmospheres*, *111*, D08S11, doi:10.1029/2005JD006017.

Gobron, N., Pinty, B., Verstraete, M. M., & Govaerts, Y. (1997). A semidiscrete model for the scattering of light by vegetation. *Journal of Geophysical Research—Atmospheres*, *102*, 9431–9446.

Gobron, N., Pinty, B., Verstraete, M. M., & Widlowski, J. L. (2000). Advanced vegetation indices optimized for up-coming sensors: Design, performance, and applications. *IEEE Transactions on Geoscience and Remote Sensing*, *38*, 2489–2505.

Govaerts, Y. M., Verstraete, M. M., Pinty, B., & Gobron, N. (1999). Designing optimal spectral indices: A feasibility and proof of concept study. *International Journal of Remote Sensing*, *20*, 1853–1873.

Harris, A., & Dash, J. (2010). The potential of the MERIS terrestrial chlorophyll index for carbon flux estimation. *Remote Sensing of Environment*, *114*, 1856–1862.

Hilker, T., Gitelson, A., Coops, N. C., Hall, F. G., & Black, T. A. (2011). Tracking plant physiological properties from multi-angular tower-based remote sensing. *Oecologia*, *165*, 865–876.

Huete, A. R., Justice, C., & van Leeuwen, W. (1996). MODIS vegetation index (mod13). Algorithm theoretical basis document. Version 2. Greenbelt, Maryland 20771. USA: NASA Goddard Space Flight Center.

Huete, A. R., Liu, H. Q., Batchily, K., & vanLeeuwen, W. (1997). A comparison of vegetation indices global set of TM images for EOS-MODIS. *Remote Sensing of Environment*, *59*, 440–451.

Jackson, R. D., Clarke, T. R., & Moran, M. S. (1992). Bidirectional calibration results for 11 spectralon and 16 $BaSO_4$ reference reflectance panels. *Remote Sensing of Environment*, *40*, 231–239.

Jordan, C. F. (1969). Derivation of leaf-area index from quality of light on forest floor. *Ecology*, *50*, 663.

Knyazikhin, Y., Martonchik, J. V., Diner, D. J., Myneni, R. B., Verstraete, M., Pinty, B., et al. (1998). Estimation of vegetation canopy leaf area index and fraction of absorbed photosynthetically active radiation from atmosphere-corrected MISR data. *Journal of Geophysical Research—Atmospheres*, *103*, 32239–32256.

Knyazikhin, Y., Martonchik, J. V., Myneni, R. B., Diner, D. J., & Running, S. W. (1998). Synergistic algorithm for estimating vegetation canopy leaf area index and fraction of absorbed photosynthetically active radiation from MODIS and MISR data. *Journal of Geophysical Research—Atmospheres*, *103*, 32257–32275.

Kohavi, R. (1995). A study of cross-validation and bootstrap for accuracy estimation and model selection. In C. S. Mellish (Ed.), *International joint conference on artificial intelligence (IJCAI)* (pp. 1137–1143). Montreal, Quebec, Canada: Morgan Kaufmann, Los Altos, CA.

Moulin, S., & Guerif, M. (1999). Impacts of model parameter uncertainties on crop reflectance estimates: A regional case study on wheat. *International Journal of Remote Sensing*, *20*, 213–218.

Myneni, R. B., Hall, F. G., Sellers, P. J., & Marshak, A. L. (1995). The interpretation of spectral vegetation indexes. *IEEE Transactions on Geoscience and Remote Sensing*, *33*, 481–486.

Myneni, R. B., Nemani, R. R., & Running, S. W. (1997). Estimation of global leaf area index and absorbed PAR using radiative transfer models. *IEEE Transactions on Geoscience and Remote Sensing*, *35*, 1380–1393.

Peng, Y., Gitelson, A., Keydan, G., Rundquist, D., & Moses, W. (2011). Remote estimation of gross primary production in maize and support for a new paradigm based on total crop chlorophyll content. *Remote Sensing of Environment*, *115*, 978–989.

Pielke, R. A., Avissar, R., Raupach, M., Dolman, A. J., Zeng, X. B., & Denning, A. S. (1998). Interactions between the atmosphere and terrestrial ecosystems: Influence on weather and climate. *Global Change Biology*, *4*, 461–475.

Pinty, B., Lavergne, T., Widlowski, J. L., Gobron, N., & Verstraete, M. M. (2009). On the need to observe vegetation canopies in the near-infrared to estimate visible light absorption. *Remote Sensing of Environment*, *113*, 10–23.

Pinty, B., Leprieur, C., & Verstraete, M. M. (1993). Towards a quantitative interpretation of spectral vegetation indexes. *Remote Sensing Reviews*, *7*, 127–150.

Rouse, J. W., Haas, R. H., Jr., Schell, J. A., & Deering, D. W. (1974). Monitoring vegetation systems in the Great Plains with ERTS. *Third ERTS-1 Symposium* (pp. 309–317). Washington, DC: NASA.

Rundquist, D., Perk, R., Leavitt, B., Keydan, G., & Gitelson, A. (2004). Collecting spectral data over cropland vegetation using machine-positioning versus hand-positioning of the sensor. *Computers and Electronics in Agriculture*, *43*, 173–178.

Running, S. W. (1990). Estimating terrestrial primary productivity by combining remote sensing and ecosystem simulation. In R. J. Hobbs, & H. A. Mooney (Eds.), *Remote sensing of biosphere functioning* (pp. 65–86). : Springer-Verlag.

Running, S. W., & Coughlan, J. C. (1988). A general-model of forest ecosystem processes for regional applications. 1. Hydrologic balance, canopy gas-exchange and primary production processes. *Ecological Modelling*, *42*, 125–154.

Sellers, P. J., Mintz, Y., Sud, Y. C., & Dalcher, A. (1986). A simple biosphere model (SiB) for use within general-circulation models. *Journal of the Atmospheric Sciences*, *43*, 505–531.

Suyker, A. E., Verma, S. B., Burba, G. G., Arkebauer, T. J., Walters, D. T., & Hubbard, K. G. (2004). Growing season carbon dioxide exchange in irrigated and rainfed maize. *Agricultural and Forest Meteorology*, *124*, 1–13.

Verma, S. B., Dobermann, A., Cassman, K. G., Walters, D. T., Knops, J. M., Arkebauer, T. J., et al. (2005). Annual carbon dioxide exchange in irrigated and rainfed maize-based agroecosystems. *Agricultural and Forest Meteorology*, *131*, 77–96.

Verstraete, M. M., Pinty, B., & Myneni, R. B. (1996). Potential and limitations of information extraction on the terrestrial biosphere from satellite remote sensing. *Remote Sensing of Environment*, *58*, 201–214.

Viña, A., & Gitelson, A. A. (2005). New developments in the remote estimation of the fraction of absorbed photosynthetically active radiation in crops. *Geophysical Research Letters*, *32*, L17403, doi:10.1029/2005GL023647.

Weiss, M., Baret, F., Leroy, M., Begue, A., Hautecoeur, O., & Santer, R. (1999). Hemispherical reflectance and albedo estimates from the accumulation of across-track sun-synchronous satellite data. *Journal of Geophysical Research—Atmospheres*, *104*, 22221–22232.

Wiegand, C. L., Richardson, A. J., & Kanemasu, E. T. (1979). Leaf area index estimates for wheat from Landsat and their implications for evapotranspiration and crop modeling. *Agronomy Journal*, *71*, 336–342.

Xiao, X., He, L., Salas, W., Li, C., Moore, B., Zhao, R., et al. (2002). Quantitative relationships between field-measured leaf area index and vegetation index derived from vegetation images for paddy rice fields. *International Journal of Remote Sensing*, *23*, 3595–3604.

Please cite this article as: Viña, A., et al., Comparison of different vegetation indices for the remote assessment of green leaf area index of crops, *Remote Sensing of Environment* (2011), doi:10.1016/j.rse.2011.08.010